Age-dependent expression and antiviral activity of interferon epsilon in respiratory epithelium

Mary McCabe[1], Helen E. Groves[1], Erin Getty[1], Emma Campbell[1], Connor G.G. Bamford[2], Guillermo Lopez Campos[1], Michael D. Shields[1], and Ultan F. Power[1*].

[1] Wellcome-Wolfson Institute for Experimental Medicine, Belfast, United Kingdom

[2] School of Biological Sciences & Institute for Global Food Security, Queen's University Belfast, Belfast, United Kingdom.

***Corresponding author**: Ultan F. Power PhD

Wellcome-Wolfson Institute for Experimental Medicine, School of Medicine, Dentistry & Biomedical Sciences, Queen's University Belfast, Medical Biology Centre, 97 Lisburn Road, Belfast BT9 7BL, Northern Ireland.

Tel: 44.28.9097.2285.

Email: u.power@qub.ac.uk

MM ORCID ID: 0000-0002-9307-5399

H.E.G ORCID ID: 0000-0001-9244-9961

E.G ORCID ID: 0009-0009-2027-7991`

C.G.G.B ORCID ID: 0000-0003-4895-1983

G.L.C ORCID ID: 0000-0003-3011-0940

M.D.S ORCID ID: 0000-0002-3793-3571

U.F.P ORCID ID: 0000-0003-3246-3774

CRediT authorship contribution statement

Mary McCabe: Writing -Original Draft, Validation, Methodology, Investigation, Formal Analysis, Data Curation. **Helen E. Groves**: Conceptualization, Methodology, Supervision. **Erin Getty**: Investigation, Writing – Review & Editing. **Emma Campbell**: Investigation. **Connor G.G Bamford**: Methodology, Resources, Writing – Review & Editing, Supervision. **Guillermo Lopez Campos**: Methodology, Conceptualization, Writing – Review & Editing, Supervision. **Michael D. Shields**: Conceptualization, Writing – Review & Editing, Funding acquisition. **Ultan F. Power**: Conceptualisation, Resources, Writing – Review & Editing, Supervision, Funding acquisition.

Declaration of competing interest

The authors declare that they have no known competing financial interests or personal relationships that could have appeared to influence the work reported in this paper.

Acknowledgements

This work was supported by Wellcome Trust grant number 104516/Z/14/Z to HG; PHA HSCNI R&D Division funding (grant numbers RRG/3244105 and Com/4044/09), and Department for Economy, Northern Ireland to UFP.

Abstract

Respiratory syncytial virus (RSV) disease burden is greatest between six weeks and 6 months of life, with young age the most common risk factor among hospitalised children. A robust innate immune response in the airway epithelium is crucial for mitigating RSV-associated disease, but early-life immune responses to infection remain largely unexplored. RNA-seq analysis of RSV-infected primary nasal epithelial cell cultures from healthy infants at birth and one year revealed diminished expression of interferon epsilon (*IFNE*), a poorly characterised type I IFN, in newborns versus one-year. We hypothesised, therefore, that *IFNE* plays an important role during infant RSV infection. We found that *IFNE* is endogenously expressed in airway epithelial cell lines. Recombinant human IFNε (rhIFNε) induced an antiviral state against an RSV clinical isolate and related Sendai virus, but not SARS-CoV-2 under the conditions tested. The antiviral potency of rhIFNε was diminished relative to rhIFN beta (rhIFNβ1) or rhIFN lambda-1 (rhIFNλ1), as evidenced by IC_{50} data. Importantly, rhIFNε induced similar ISGs as rhIFNβ1 but demonstrated a transient temporal expression profile that differed from both rhIFNβ1 and rhIFNλ1. These results suggest that lower IFNε expression at birth may contribute to increased susceptibility to severe RSV-associated disease, offering insights into potential therapeutic interventions.

Keywords

Respiratory Syncytial Virus, Innate Immunity, Interferons, Interferon Epsilon, Sendai Virus, SARS-CoV-2

62 **Introduction**

63 Respiratory syncytial virus (RSV), a single-stranded negative-sense RNA virus of the
64 *Pneumoviridae* family and *Orthopneumovirus* genus, is the commonest cause of acute lower
65 respiratory tract infection (ALRTI) in infants globally [1]. Annually, ~33 million RSV LRTIs occur in
66 children <5 years old, resulting in ~101,400 infant deaths [1]. Despite recent pharmacological
67 advancements [2–6], treatment for severe RSV-associated disease remains palliative, with no
68 RSV-specific antivirals or direct vaccination available for infants <6 months, the age group in
69 which the disease burden is greatest [1, 7]. While epidemiological data has identified risk factors
70 [8–14], most infants hospitalised share only the risk factor of age, suggesting host intrinsic
71 features predispose them to severe disease. Because of the current incomplete understanding
72 of RSV-host interactions in early life, we cannot predict which infants will experience severe
73 disease and, thereby, prioritise prophylactic treatment. As RSV initially targets the ciliated cells
74 of the nasopharynx [15–17], efficient innate immune responses play a vital role in determining
75 RSV infection outcomes. Yet, whether and how these responses develop over time, and why
76 infants <6 months are more frequently susceptible to severe disease, is unknown.

77 Interferons (IFN) are a crucial innate barrier against viral infection and dissemination [18, 19]. In
78 the respiratory epithelium, type I (IFNα and -β) and type III (IFNλ1-λ4) IFNs play significant roles.
79 Recently, Taveras *et al,* determined that all IFN types (I, II and III) from nasal samples were
80 significantly increased in children (>6 years) versus infants (<6 months) and higher in milder
81 outpatient RSV infections compared to severe inpatient infections [20]. Furthermore, we
82 observed a threefold increase in mean IFNλ1 protein secretion at one year versus birth within
83 paired birth and one-year primary nasopharyngeal cell samples (unpublished data, Groves HE,
84 McCabe M, Coey J, Broadbent L, Guo-Parke H, Lopez Campos G, et al). These results suggest that
85 strong IFN responses are a critical component of determining disease severity. As such, more

86 robust IFN responses to RSV infection with increasing chronological age may contribute to
87 protection against severe disease in older infants and adults.

88 IFN epsilon (*IFNE*/IFNε) is a highly conserved type I IFN recognised for its multifaceted
89 antimicrobial properties in the female reproductive tract (FRT) and its expression at other
90 mucosal interfaces, including the lungs [21–24]. In contrast to other type I IFN subtypes, IFNε is
91 100-1000-fold less potent, and is expressed at high levels basally [25–27]. Interestingly, Thwaites
92 *et al* described a trend for increased expression of type I IFNs (*IFNA1*, *IFNB1* and *IFNE*) in infants
93 with moderate RSV ALRTI relative to severe cases [28] and *IFNE* was upregulated in children and
94 young adults with SARS-CoV-2 infection [29]. Furthermore, *IFNE* was observed to be differentially
95 expressed in children with long-coronavirus disease (COVID) symptoms [30]. Therefore, despite
96 its conserved mucosal antiviral activity, understanding of the local expression and function of
97 IFNε in airway epithelium against respiratory viruses, and its possible contributions to viral
98 disease severity, remain limited.

99 In this study, we identified for the first time *IFNE* as differentially expressed with chronological
100 age and confirmed its endogenous expression in immortalised airway epithelial cells. We
101 assessed its antiviral activity against a clinical isolate of RSV and a related RNA virus, Sendai
102 virus, and SARS-CoV-2. We determined the IC_{50} concentration of rhIFNε against RSV compared
103 to other relevant mucosal IFNs and characterised the induction of downstream interferon-
104 stimulated genes (ISGs). These results suggest an underappreciated role of IFNε in the induction
105 of protective antiviral responses in the respiratory epithelium.

106

107

108

109

110 **Materials and Methods**

111 Cell Culture

112 BEAS-2B cells (kindly provided by Cliff Taggart, Queen's University Belfast) were maintained in 1
113 g/L (low) glucose DMEM with 10 units/mL Pen/Strep and 5% FBS. HEp-2 cells (kindly provided by
114 Prof. Ralph Tripp, University of Georgia) were maintained in 4.5 g/L (high) glucose DMEM with 10
115 units/mL Pen/Strep and 5% FBS. A549, Vero E6 and Vero's expressing ACE2 and TMPRSS2 (VAT)
116 cells were maintained in 4.5 g/L (high) glucose DMEM with 10 units/mL Pen/Strep and 10% FBS.
117 A549 expressing human ACE2 and TMPRSS2 (AAT) cells were maintained in 4.5 g/L (high) glucose
118 DMEM with 10 units/mL Pen/Strep, 10% FBS and maintained under antibiotic selection with
119 Hygromycin B (25 ug/mL) and Geneticin (25 ug/mL).

120 Nasal brushings were performed on healthy newborn term infants, (37–42 weeks gestation) and
121 preterm infants (28–34 weeks gestation) at birth and repeated in the same infants at one-year-
122 old, as previously described [31]. Harvested paediatric nasal cells were cultured to
123 differentiation using established methods [16][32] and infected with Multiplicity of Infection
124 (MOI) 3 in duplicate with a clinical isolate of RSV, designated BT2a, or mock-infected as previously
125 described [33].

126 RNA-Seq

127 Total RNA was extracted from WD-PNEC cultures at 96 hpi (High pure RNA isolation kit, Roche
128 diagnostics, Indianapolis, USA) and RNA quality was determined (Agilent RNA 6000 Nano Kit)
129 using the 2100 Bioanalyzer Instrument (Agilent Technologies). Total RNA sequencing was
130 conducted (unpublished data, Groves HE, McCabe M, Coey J, Broadbent L, Guo-Parke H, Lopez
131 Campos G, et al).

132 Virus Stocks and Titrations

133 RSV BT2a (clinical isolate) was isolated and characterised as previously described [33]. RSV
134 A2/mkate2 (a recombinant RSV reporter virus expressing Katushka, a far-red fluorescent protein)
135 was rescued from an infectious clone and helper plasmids kindly provided by Dr Martin Moore
136 (Emory University, Atlanta, USA). Sendai virus/eGFP (rSeV/eGFP) was generated by reverse
137 genetics [34]. SARS-CoV-2 Delta Variant was isolated from nasal swabs [35]. EMCV-Rueckert was
138 obtained as described previously [36]. Viral infections were performed at the MOI stated in each
139 figure legend by adding diluted virus suspensions to the apical compartment of WD-PNECs or
140 directly onto cell lines in serum-free medium. HEp-2 cells were used to titrate RSV BT2a, and Vero
141 E6 cells were used to titrate EMCV by tissue culture infectious dose 50 ($TCID_{50}$) assays. SARS-
142 CoV-2 plaque assays were performed on VAT cells [35].

143 RNA extraction and RT-qPCR

144 RNA was extracted according to the manufacturer's instructions (High pure RNA isolation kit,
145 Roche) and RNA quality was determined (Nanodrop One, Thermo Scientific®). cDNA synthesis
146 was performed in a 96-well thermocycler (Bio-Rad) using a High-Capacity cDNA Reverse
147 Transcription Kit (Applied Biosystems), according to the manufacturer's instructions. For the
148 target genes, *IFNE* (assay ID Hs00703565_s1*), IFNL1* (assay ID Hs00601677_g1), *IFNB1* (assay ID
149 Hs01077958_s1)*, MX1* (assay ID Hs00895608_m1)*, ISG15* (assay ID Hs01921425_s1)*, IFIT1*
150 (assay ID Hs03027069_s1)*, RSDA2* (assay ID Hs00369813_m1)*, IRF1* (assay ID Hs00971965_m1),
151 *CXCL10* (assay ID Hs00171042_m1), YWHAZ (assay ID Hs01122445_g1), TBP (assay ID
152 Hs00427620_m1) and IPO8 (assay ID Hs00914057_m1) Thermo Fischer Scientific TaqMan ready-
153 to-use primer/probes were purchased and employed with the LightCycler 480 Probes Master Mix
154 (Roche). Relative quantification analysis of gene expression was performed using LightCycler 96
155 software (Roche). The Relative Quantification Cycle (Cq) of the sample was determined by
156 comparing the target gene to 3 reference housekeeping genes: *YWHAZ*, *TBP*, and *IPO8*.

157 Recombinant human protein

158 Cell lines were pretreated with recombinant human interferon epsilon (rhIFNε) (R&D systems,
159 Minneapolis, MN, USA), rhIFN beta (rhIFNβ1) (Peprotech®) and rhIFN lambda-1 (rhIFNλ1)
160 (Peprotech®) in low-serum DMEM for intervals stated within each figure legend. Cells were then
161 infected in serum-free DMEM. Following infection, cells were incubated for 2 h at 37 °C. After 2
162 h, the viral inoculum was removed and washed three-times with serum-free DMEM to remove
163 unattached virus, low-serum DMEM replaced and incubated at 37°C.

164 Cell Imaging and Analysis

165 The mean % fluorescence ratio of RSV A2/mkate2 and rSeV/eGFP infected cells was measured
166 using the brightfield and red/green fluorescence channels of the Celigo Imaging Cytometer
167 (Nexcelom). All data were presented as % fluorescence ratio ((brightfield confluence/red or green
168 confluence) *100).

169 Generation of BEAS-2B IFNLR1$^{-/-}$ cells

170 BEAS-2B cells overexpressing Cas9 were generated via lentiviral transduction of a third
171 generation lentiviral Cas9 expression plasmid (Addgene #52962), blasticidin selection (10 ug/mL)
172 and single-cell clonal isolation. Western blotting was used to confirm the stable expression of
173 Cas9 (Sigma-Aldrich, F3165). To generate *IFNLR1* BEAS-2B clonal cell line knockouts, a single-
174 guide RNA (sgRNA) (priCRISPR.IFNLR1.1(+) CACCGGTATTCGGACTCCACCCAG) was designed.
175 For each sgRNA, a forward and reverse oligonucleotide sequence was synthesised (Eurofins),
176 annealed and inserted into the lentiGuide-Puro vector via BsmB1-v2 (NEB) restriction digestion
177 and T4 DNA ligase (NEB) mediated ligation. Vector-sgRNA DNA was then transformed into DH10B
178 competent cells (Thermo Fischer Scientific) and spread onto Ampicillin selection plates (50
179 mg/mL). Single colonies were picked and miniprepped using PureLink™ HiPure Plasmid Miniprep
180 kit according to manufacturer's instructions (Invitrogen™). BEAS-2B *IFNLR1* knockout cell lines
181 were generated via lentiviral transduction of a third generation lentiGuide-Puro plasmid (Addgene

182 #84752) with inserted sgRNA sequence, puromycin (Gibco) selection and single-cell clonal
183 isolation.

184 Statistical Analysis

185 Statistical analyses included an unpaired two-tailed Student's t-test and one-way analysis of
186 variance (ANOVA) to assess the significance of test conditions, as stated in the figure legends.
187 For the time course profiles we calculated the Area under Curve (AUC) and then used this
188 summary measure for comparisons using one-way ANOVA. Statistical analysis was set at *
189 $p<0.05$, ** $p<0.01$, ***$p<0.001$, ****$p<0.0001$. Data presented as means ± standard error of the
190 means (SEM). Data were analysed using GraphPad® Prism 10 (GraphPad Software, Inc, La Jolla,
191 CA).

192 Data Availability

193 RNA-seq data has been deposited under moratorium pending publication and will be made
194 available to reviewers upon request. The GEO accession number for the RNA-seq data is:
195 GSE231666.

196

197

198

199

200

201

202

203

204 **Results**

205 **Endogenous expression of *IFNE* increases during the first year of life.**

206 In a recent study, we evaluated the impact of gestational and chronological age on RSV-induced
207 airway epithelium innate immune responses using RNA-Seq (unpublished data, Groves HE,
208 McCabe M, Coey J, Broadbent L, Guo-Parke H, Lopez Campos G, et al) (**Figure 1A**). RNA-seq
209 analysis of RSV-infected WD-PNECs derived from infants sampled at birth and one-year-old
210 revealed 63 differentially expressed genes (DEGs) (42 upregulated, 21 downregulated) with
211 Log2Fold >|2| when comparing RSV-induced responses from 1-year- versus newborn-derived
212 cultures (**Figure 1B**). Included in the 42 upregulated DEGs, *IFNE,* a poorly characterised type I
213 IFN, was significantly increased following RSV infection versus uninfected controls (**Figure 1C**).
214 Furthermore, *IFNE* expression was higher in 1 year- versus newborn-derived WD-PNECs, both at
215 baseline and following RSV infection (**Figure 1C**). These results suggested that *IFNE* may play an
216 unappreciated antiviral role in respiratory airway epithelium and contribute to more robust
217 antiviral activities at 1 year compared to newborns.

218

219

220

221

222

223

224

225

226

227

228

229

230 **A.**

231

232

233

234

235

236

237

238

239

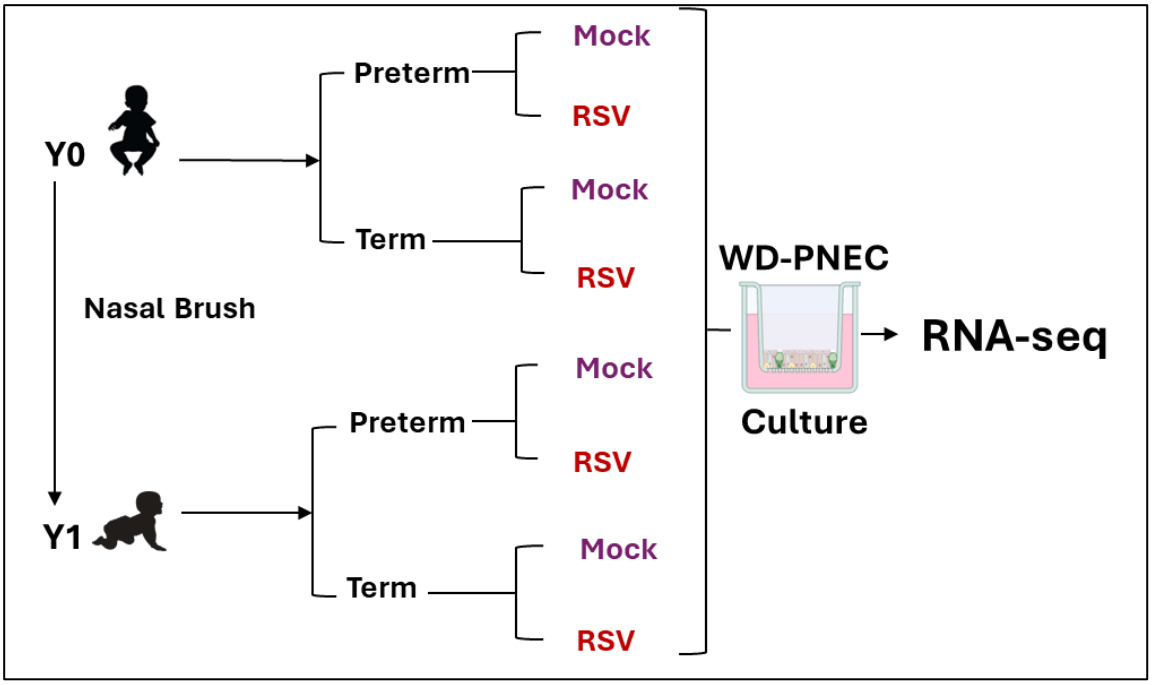

240

B.

241

242

243

244

245

246

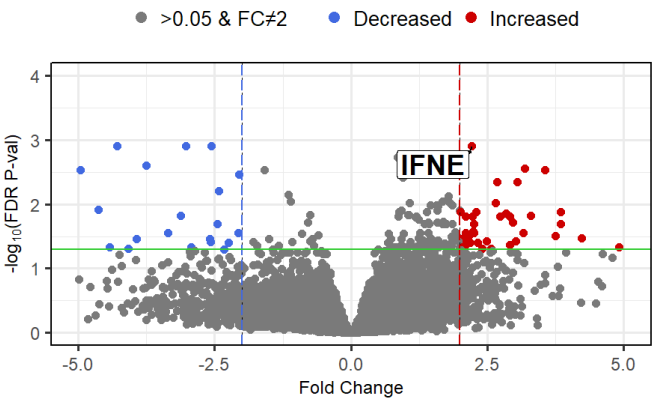

C.

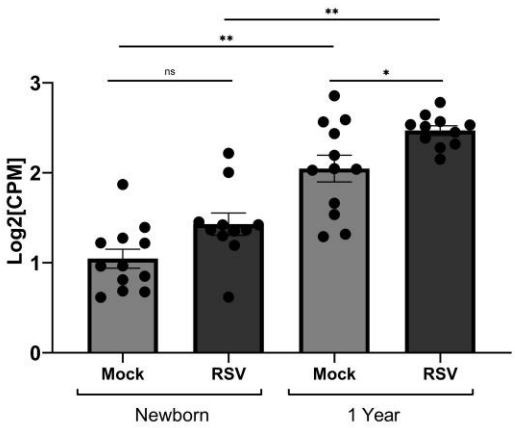

247 **Figure 1. Increase in *IFNE* expression during the first year of life.** (**A**) Summary of RNA-Seq experimental set-up. WD-PNEC cultures (n=12 paediatric donors) were infected with clinical isolate RSV BT2a (MOI=3) or mock-infected. RNA was extracted at 96 hpi and total RNA sequencing was conducted. (**B**) Volcano plot displaying differentially

248 expressed genes associated with RSV-infected cultures from 1-year-old and newborn donors, with *IFNE* expression highlighted. X-axis depicts the log2 differences in gene expression for each comparison of interest, with positive

249 values (in red) displaying significantly increased gene expression (log2 FC ≥ 2) and negative values (in blue) displaying significantly decreased gene expression (log2 FC ≤ -2). Y axis depicts adjusted p values (-log10 scale) for

250 each gene (higher p values representing greater statistical significance) after adjusting for batch by the year RNA-sequencing was completed. Green horizontal line indicates 0.05 p-value significance cut-off (**C**) *IFNE* Log2 Counts per Million (CPM). Statistical analyses were corrected for multiple testing by applying the Benjamini-Hochberg (BH)

251 p value correction (* p<0.05, ** p<0.01).

252

253

254 **Endogenous expression of *IFNE* in immortalised airway epithelial cells.**

255 Next, we assessed the expression of *IFNE* and two other mucosal IFNs within airway epithelial
256 cells, including a type I (*IFNB1)* and a type III IFN (*IFNL1)*. *IFNB1* was chosen as a comparator as
257 it was the sole type I IFN differentially expressed with infection within the RNA-seq data
258 (unpublished data, Groves HE, McCabe M, Coey J, Broadbent L, Guo-Parke H, Lopez Campos G,
259 et al). *IFNλ1* was chosen as a representative type III IFN as our group showed increased IFNλ1
260 release from primary cultures derived from infant respiratory tract samples following RSV
261 infection [37]. Within common airway epithelial cell lines used to model RSV infection, *IFNE* was
262 constitutively expressed at low levels, with the highest expression in adenocarcinoma human
263 alveolar basal cells (A549) and A549 cells over-expressing human ACE2 and TMPRSS2 (AAT)
264 (**Figure 2A**). Low levels of expression were evident in immortalised human bronchial epithelial
265 cells (BEAS-2B) and human laryngeal carcinoma cells (HEp-2) (**Figure 2A**). This contrasted with
266 *IFNB1* and *IFNL1*, which exhibited negligible expression under unstimulated sterile cell-culture
267 conditions (**Figure 2B-C**). To further characterise *IFNE* expression, we infected A549 (**Figure 2D-**
268 **F**) and BEAS-2B (**Figure 2G-I**) cells with a recombinant RSV reporter virus expressing a far-red
269 fluorescent protein (RSV-A2/mKate2) or mock-infected them. At 48 hpi *IFNE*, *IFNB1* and *IFNL1*
270 mRNA expression was higher within A549 cells (**Figure 2E-F**) compared to BEAS-2B cells (**Figure**
271 **2H-I**). *IFNE* expression was detected irrespective of infection in both cell lines (**Figure D, G**), with
272 this unique endogenous pattern emphasized when comparing its expression to that of *IFNB1* or
273 *IFNL1*.

274

275

276

277

278

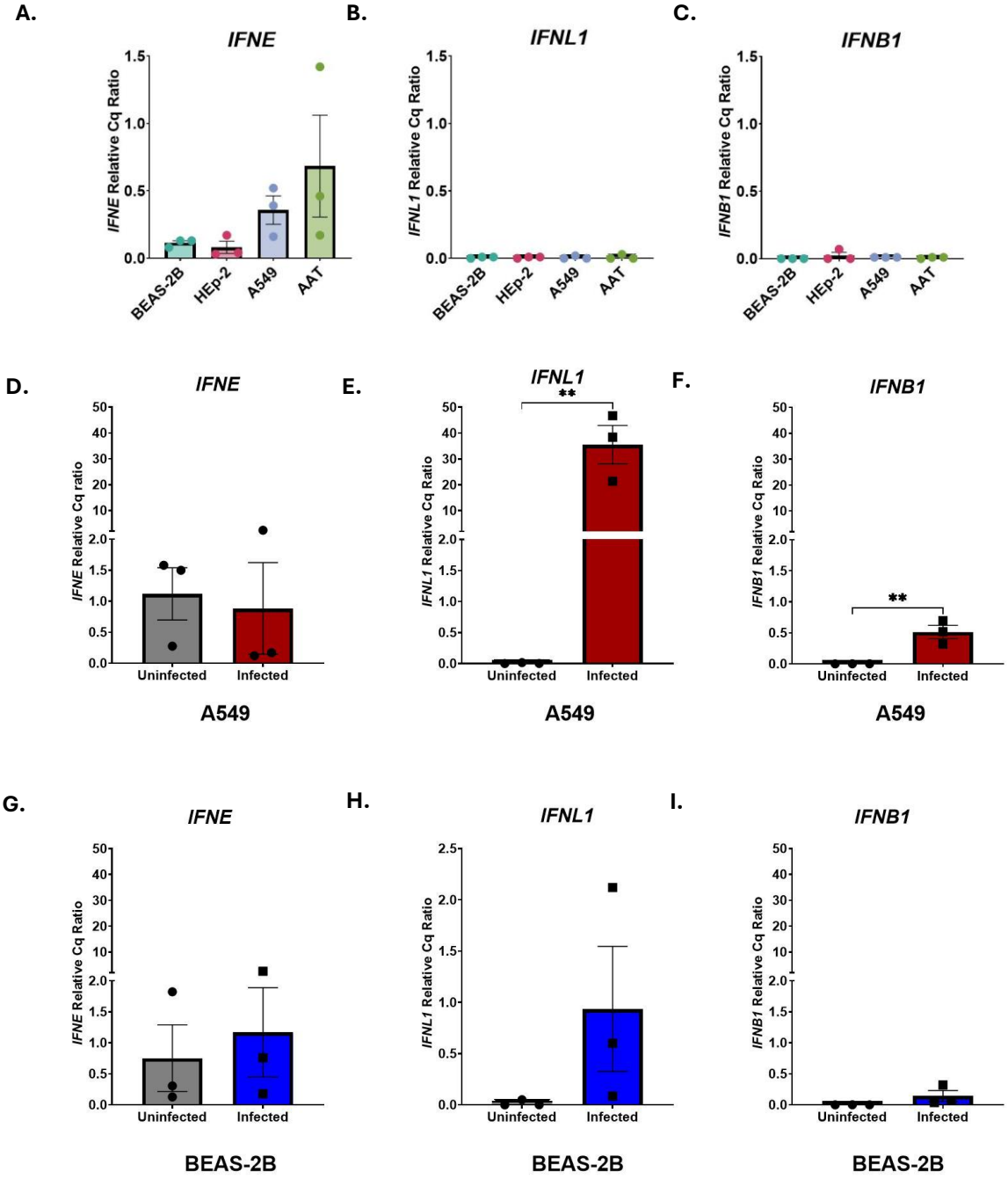

Figure 2. *IFNε* is endogenously expressed in immortalised airway epithelial cells. BEAS-2B, A549, AAT and HEp-2 cells were seeded in 24 well plate. 24 h post seeding total RNA was extracted, reverse transcribed and subjected to qPCR analysis from BEAS-2B, A549, AAT and HEp-2 cells for *IFNE*, *IFNL1* and *IFNB1* expression (ROCHE, Lightcycler 480). Graphs show relative ratio values for (**A**) *IFNE*, (**B**) *IFNL1* and (**C**) *IFNB1* normalised using *YWHAZ*, *IPO8* and *TBP* as house-keeping genes. Data are presented as mean of triplicate technical replicates (±SEM) for n=3 independent experiments. (**D-F**) A549 or (**G-I**) BEAS-2B cells were mock-infected or infected with RSV-A2/mKate2 (MOI 1). At 48 hpi total RNA was extracted, reverse transcribed and subjected to qPCR analysis of *IFNE*, *IFNL1* and *IFNB1* expression (ROCHE, Lightcycler 480). Graphs show relative ratio values for *IFNE*, *IFNL1* and *IFNB1* normalised using *YWHAZ*, *IPO8* and *TBP* as housekeeping genes. Data are presented as the mean of duplicate technical replicates (±SEM) for n=3 independent experiments at 48 hpi. Statistical analyses were conducted using an unpaired two-tailed Student's t-test (* $p<0.05$, ** $p<0.01$).

285 **IFNε has antiviral activity against RSV that is concentration- and cell type-dependent.**

286 To assess if recombinant human IFNε (rhIFNε) protein can induce an antiviral effect within airway
287 epithelial cell lines, A549 (**Figure 3A**) and BEAS-2B (**Figure 3B**) cells were pre-treated with rhIFNε,
288 rhIFNβ1 and rhIFNλ1 protein (100 ng/mL) and infected with the highly IFN-sensitive virus
289 encephalomyocarditis virus (EMCV) (MOI 1). IFNε pretreatment resulted in a 1.15-$\log_{10}$ reduction
290 in EMCV titre versus the untreated in BEAS-2B cells (**Figure 3A**). This was similar to rhIFNλ1
291 pretreatment (1.7-log reduction) but much less effective than rhIFNβ1 pretreatment (3.5-$\log_{10}$
292 reduction). There was a non-statistically significant trend towards a reduction in virus titres
293 within A549 cells (**Figure 3B**).

294 To explore the antiviral activity of rhIFNε against RSV, BEAS-2B (**Figure 3C**), HEp-2 **(Figure 3D**),
295 A549 (**Figure 3E)** and AAT (**Figure 3F**) cells were pretreated with rhIFNε at a range of doses (100,
296 50, 5, 0.5 and 0.05 ng/mL) and infected with RSV-A2/mKate2 (MOI=0.3). A range was selected, as
297 prior to this study, there was no evidence of IFNε's antiviral effect against respiratory viruses,
298 including, but not limited to, RSV. At 24 hpi, the mean % fluorescence ratio was measured using
299 the brightfield and red fluorescence channels of the Celigo Imaging Cytometer (Nexcelom). BSA
300 pretreatment (5 μg/mL) was a negative control for the recombinant protein stabilisation carrier,
301 and rhIFNβ1 and rhIFNλ1 pretreatment (100 ng/mL) were used as positive controls to ensure cell
302 responsiveness to IFNs. Using fluorescence as a surrogate marker of viral replication, rhIFNε
303 pretreatment resulted in a significant reduction in virus fluorescence in BEAS-2B (**Figure 3C**) and
304 HEp-2 cells (**Figure 3D**), but not in A549 or AAT cells (**Figure 3E-F**), although there was a trend
305 towards reduction in the latter cell lines. Reduction in virus replication was dose-dependent, with
306 100 ng/mL of rhIFNε resulting in the greatest reduction compared to untreated controls (1.8-fold
307 reduction) in the most responsive cell line (BEAS-2B) (**Figure 3C**). This was less potent than
308 rhIFNβ1 (27-fold reduction) but similar to rhIFNλ1 (1.9-fold reduction) (**Figure 3C**). RSV-
309 A2/mKate2 fluorescence was much lower in AAT cells (**Figure 3F**) compared to their parental

310 counterpart A549 cells. To assess the antiviral effect against RSV BT2a [33], BEAS-2B cells were
311 pre-treated with 100 ng/mL of rhIFNε, rhIFNβ1and rhIFNλ1 and infected with RSV BT2a (MOI 0.3).
312 BEAS-2B cells were selected as they are a non-tumour transformed cell line and more responsive
313 to IFN stimulation. We found a 0.37-Log_{10} reduction at 24 hpi (**Figure 3G**) in RSV titres in rhIFNε
314 pre-treated cells compared to untreated controls. A similar reduction was seen with rhIFNβ1
315 (0.39-Log_{10} reduction) and rhIFNλ1 (0.44-Log_{10} reduction) pre-treatment at 24 hpi. Thereafter,
316 while mean virus growth kinetics were delayed slightly at 48 hpi, titres at 72 and 96 hpi were
317 indistinguishable from untreated- or BSA-controls (**Figure 3H**).

318

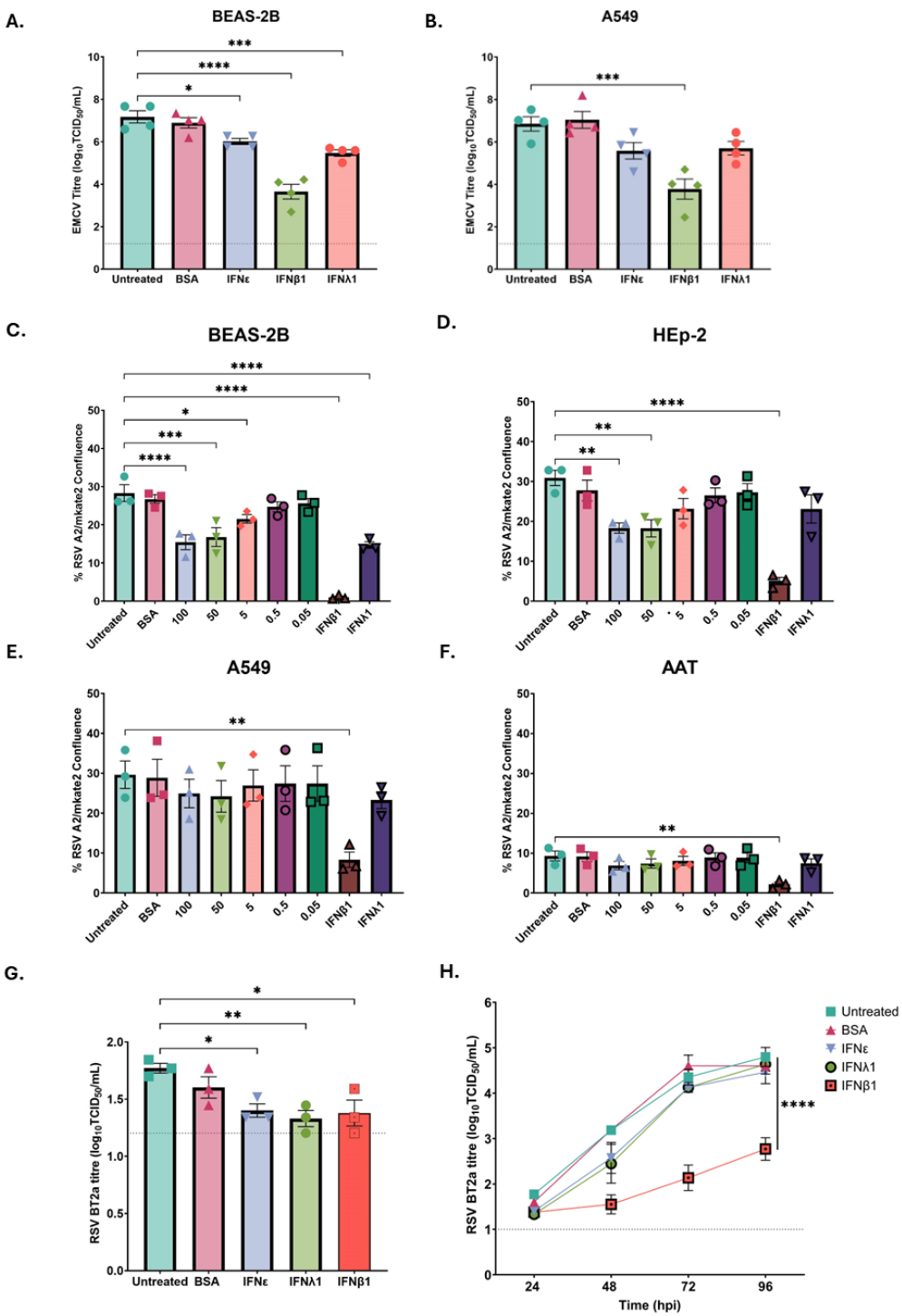

Figure 3. IFNε pretreatment reduces EMCV and RSV replication in BEAS-2B cells. (A) A549 and (**B**) BEAS-2B cells were pre-treated for 16 h with an IFN (100 ng/ml). Cells were then infected with EMCV (MOI=1) for 2 h at 37°C. Data are presented as mean of duplicate technical replicates (±SEM) for n=4 independent experiments. Statistical analysis was conducted using one-way ANOVA. (**C**) BEAS-2B, (**D**) HEp-2 (**E**) A549, and (**F**) AAT cells were pre-treated for 16 h with IFNε (100, 50, 5, 0.5, and 0.05 ng/mL), IFNβ1 or IFNλ1 (100 ng/mL). Cells were then infected with RSV-A2/mKate2 (MOI=0.3). (C-F) At 24 hpi mean % fluorescence ratio was measured using the brightfield and red fluorescence channels of the Celigo Imaging Cytometer (Nexcelom). Data presented as % fluorescence ratio for mean of triplicate technical replicates (±SEM) n=3 independent experiments. Statistical analysis (C-F) was conducted using one-way ANOVA. (**G-H**) BEAS-2B cells were pre-treated for 16 h with 100 ng/mL of IFN. Cells were then infected with RSV BT2a (MOI=0.3). Supernatants were collected at 24, 48, 72, and 96 hpi and $TCID_{50}$ assays were conducted to determine RSV titres. Data are presented as the mean of duplicate technical replicates (±SEM) log_{10} $TCID_{50}$/mL at (**G**) 24 hpi and a (**H**) 24-96 hpi time course for n=3 independent experiments. Statistical analysis for (**G**) was conducted using one-way ANOVA and for (**H**) using one-way ANOVA of AUC (* p<0.05, ** p<0.01, ***p<0.001, ****p<0.0001).

323 **Relative antiviral activity of IFNε, IFNλ1 and IFNβ1 against RSV.**

324 To further facilitate meaningful comparisons of the relative antiviral activity of rhIFNε with
325 rhIFNβ1 and rhIFNλ1, we determined the half-maximal inhibitory concentration (IC_{50}) of these
326 IFNs against RSV in BEAS-2B cells. Cells were pre-treated with decreasing concentrations of
327 rhIFNε (**Figure 4A**), rhIFNλ1 (**Figure 4B**) and rhIFNβ1 (**Figure 4C**) and infected with RSV-
328 A2/mKate2 (MOI=0.1). As anticipated, IFNε possessed the highest best-fit IC_{50} value (9 ng/mL),
329 followed by IFNλ1 (2.8 ng/ml) and IFNβ1 (0.24 ng/mL).

330 Given the limited understanding of how IFNε exerts its antiviral activity, we aimed to confirm
331 that its presence would not interfere with the activity of other type I IFNs, specifically IFNβ1,
332 in our study. Therefore, to further explore this without the interference from type III IFNs,
333 *IFNLR1*$^{-/-}$ BEAS-2B cells (**Figure 4D**) were either pre-treated (**Figure 4E-F**), treated at infection
334 (**Figure 4G-H)** or at 2 h post-infection (**Figure 4I-J**) with the IC_{50} concentrations (**Figure 4E,**
335 **G, I**) or 100 ng/mL (**Figure 4F, H, J**) of rhIFNε and rhIFNβ1. Cells were infected with RSV-
336 A2/mKate2 (MOI=0.1). At 24 hpi, IC_{50} concentrations of rhIFNε and rhIFNβ1 resulted in a
337 reduction in viral spread with pre-treatment and with treatment at infection (**Figure 4E-H**).
338 However, IC_{50} concentrations of rhIFNε and rhIFNβ1 were not sufficient to significantly
339 diminish RSV spread when treatment commenced 2 hpi (**Figure 4I)**. When pre-treated with
340 both IFNs sequentially (rhIFNε and then rhIFNβ1 or vice versa) or treated with a combination
341 of the two IFNs at the same time, the antiviral activity of rhIFNβ1 was not altered in the
342 presence of rhIFNε. The greatest reduction in virus spread was seen when rhIFNβ1 was
343 present regardless of the sequence of addition. Cells pre-treated or treated at infection with
344 100 ng/mL resulted in robust inhibition of viral spread, with those treated with 100 ng/mL
345 rhIFNβ1 showing the greatest reduction (**Figure F-H**). Only 100 ng/mL of rhIFNβ1 inhibited
346 viral spread significantly with treatment post-infection (**Figure 4J**). rhIFNλ1 pre-treatment
347 (100 ng/mL) in *IFNLR1*$^{-/-}$ BEAS-2B cells did not result in a significant reduction in virus spread

348 (**Figure 4J**). These results demonstrated that rhIFNε does not interfere with the antiviral

349 activity of rhIFNβ1, despite both binding to the same receptor, at IC_{50} concentrations or 100

350 ng/mL.

351

352

353

354

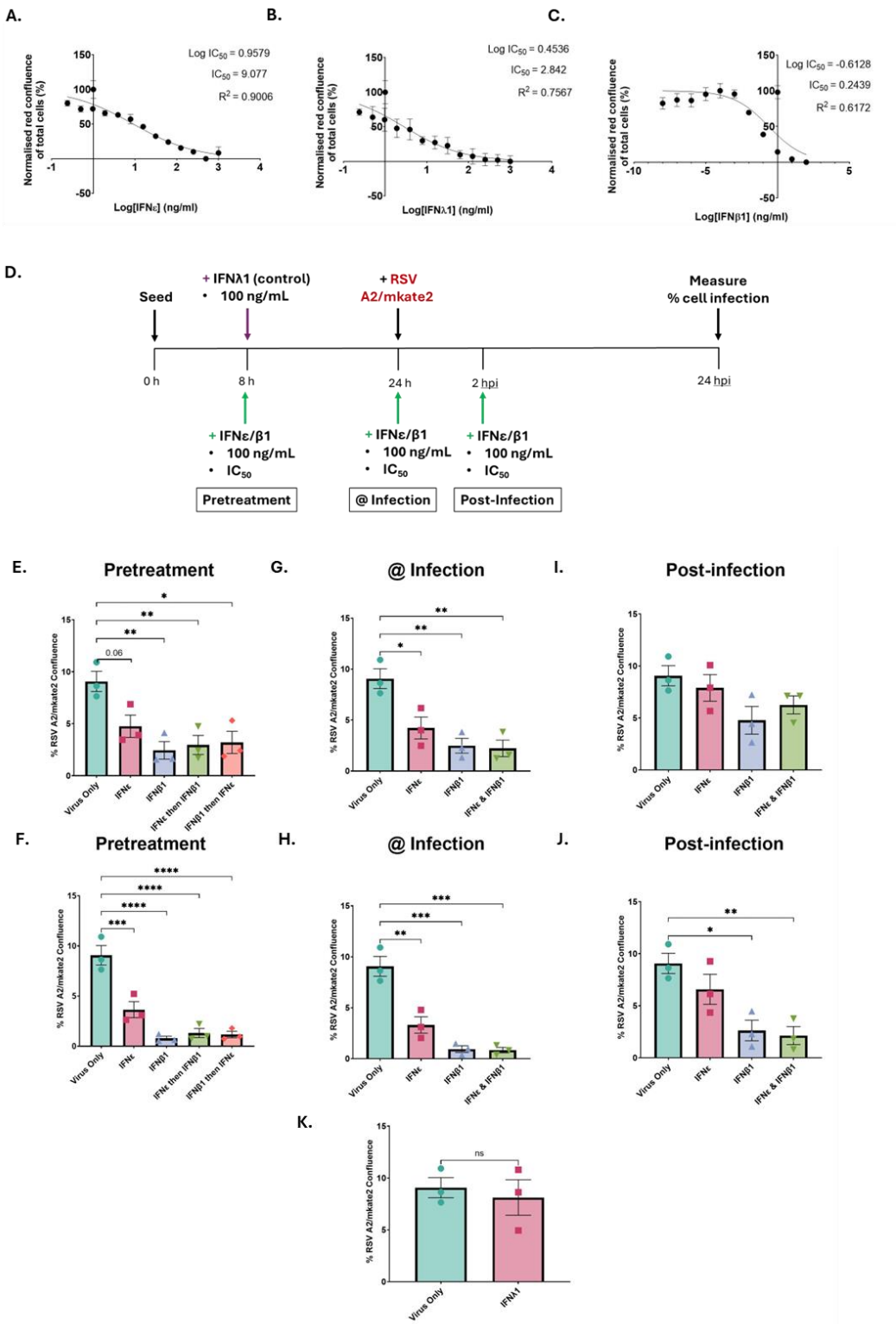

Figure 4. IFNε possesses an increased IC_{50} concentration against RSV compared to IFNβ1. BEAS-2B cells were pre-treated for 16 h with decreasing concentrations of (**A**) IFNε, (**B**) IFNλ1 and (**C**) IFNβ1. Cells were then infected with RSV-A2/mKate2 (MOI=0.1). At 24 hpi mean % fluorescence ratio was measured using the brightfield and red fluorescence channels of the Celigo Imaging Cytometer (Nexcelom). Statistical analysis (**A-C**) was conducted fitting a non-linear dose-response curve for mean of triplicate technical replicates for n=2 (IFNε and IFNλ1) or n=3 (IFNβ1) independent experiments in triplicate. (**D**) Summary of Experimental set-up for pretreatment, treatment at infection and treatment post-infection experiment. *IFNLR1* Cas9 knockout BEAS-2B cells were either pretreated (**E-F**), treated at infection (**G-H**) or treated 2 hours post infection (**I-J**) with the IC_{50} concentration (**E**, **G**, **I**) or 100 ng/mL (**F**, **H**, **J**) of recombinant human IFNε and IFNβ1 protein. Cells were infected with RSV-A2/mKate2 (MOI=0.1). (**K**) *IFNLR1*$^{-/-}$ BEAS-2B cells pretreated with 100 ng/mL of recombinant human IFNLR1. Data presented as % fluorescence ratio for as the mean of triplicate technical replicates (±SEM) n=3 independent experiments. Statistical analysis was conducted using one-way ANOVA (* p<0.05, **p<0.01, ***p<0.001, ****p<0.0001).

359 **IFNε induces antiviral activity against Sendai Virus but not SARS-CoV-2.**

360 To assess if an antiviral effect was evident beyond EMCV and RSV, A549 (**Figure 5A**) and BEAS-2B
361 (**Figure 5B**) cells were pre-treated with a dose range of rhIFNε (100, 50, 5, 0.5 and 0.05 ng/mL)
362 and infected with rSeV/eGFP (MOI=0.3). No significant reduction was observed in A549 cells,
363 despite a reduction trend being observed (**Figure 5A**). At 24 hpi, a similar dose-dependent
364 antiviral activity of rhIFNε was evident against rSeV/eGFP, as previously described for RSV
365 A2/mkate2 in BEAS-2B cells (**Figure 5B**). The antiviral effect of rhIFNε pre-treatment (2.2-fold
366 reduction) was like that of rhIFNλ1 (4-fold reduction) in BEAS-2B cells but less impressive
367 compared to rhIFNβ1 (16.3-fold reduction) (**Figure 5B**). In contrast, AAT cells pretreated with
368 rhIFNε, rhIFNβ1 or rhIFNλ1 (100 ng/mL) and infected with the SARS-CoV-2 Delta variant
369 (MOI=0.3), had no significant reductions in viral replication with IFNε pre-treatment, a slight but
370 significant reduction in virus replication with rhIFNλ1 pre-treatment, and a complete abrogation
371 of virus replication following rhIFNβ1 pre-treatment at 48 hpi (**Figure 5C**) and over a time course
372 of infection (**Figure 5D**). These results suggest that rhIFNε possesses antiviral activity against
373 some RNA viruses, but not SARS-CoV-2 Delta Variant, at least at the dose tested, and its potency
374 is clearly reduced compared to rhIFNβ1.

375

376

377

378

379

380

381

382

383

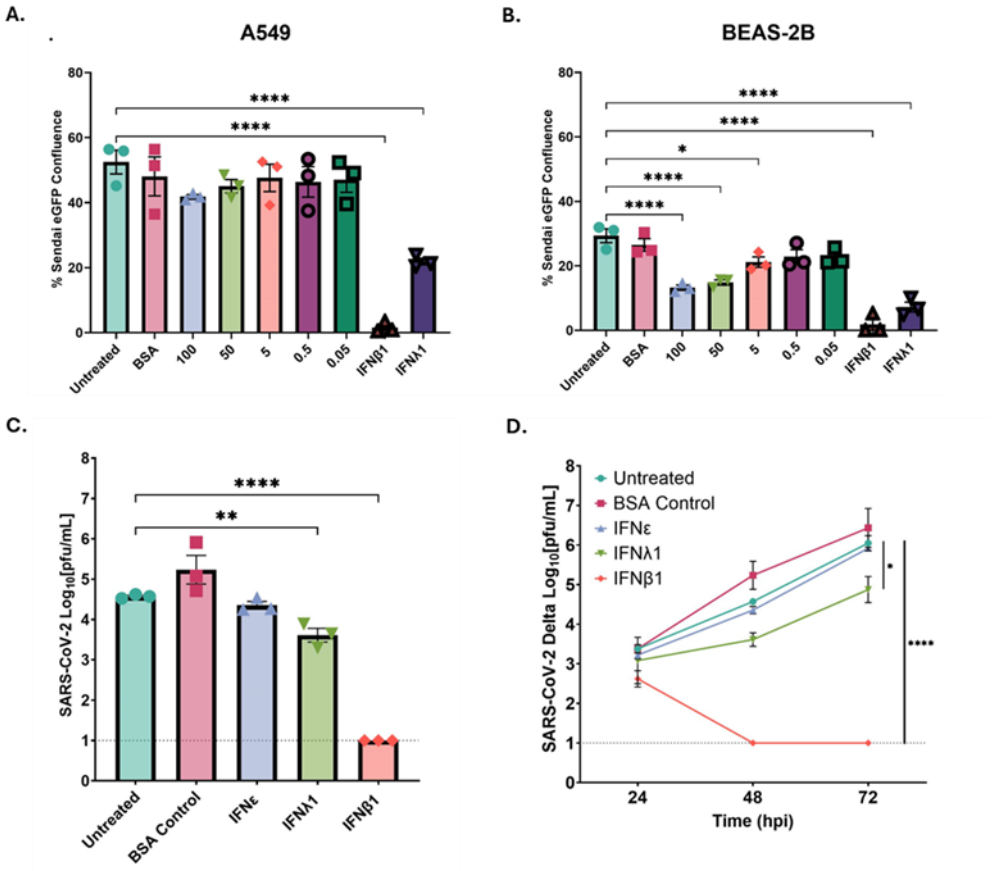

Figure 5. Relative potency of IFNε, IFNλ1 and IFNβ1 pre-treatment against Sendai virus and SARS-CoV-2. (**A**) A549 and (**B**) BEAS-2B cells were pre-treated for 16 h with IFNε (100, 50, 5, 0.5, and 0.05 ng/ml), rhIFNβ1 or rhIFNλ1 (100 ng/mL). Cells were infected with rSeV/eGFP (MOI=0.3). At 24 hpi mean % fluorescence ratio was measured using the brightfield and green fluorescence channels of the Celigo Imaging Cytometer (Nexcelom). Data presented as % fluorescence ratio for mean of triplicate technical replicates (±SEM) for n=3 independent experiments. Statistical analysis was conducted using one-way ANOVA. (**C-D**) AAT cells were pre-treated for 16 h with rhIFNε, rhIFNλ1 and rhIFNβ1 (100 ng/mL). Cells were then infected with SARS-CoV-2 Delta variant (MOI=0.3). Supernatants were collected at 24, 48, and 72 hpi and plaque assays were performed on VATs. Data presented as the mean of triplicate technical replicates (±SEM) $\log_{10}$ pfu/mL at (**C**) 48 hpi and a (**D**) 24-72 hpi time course for n=3 independent experiments. Statistical analysis (**C**) was conducted using one-way ANOVA (**D**) Statistical analysis was conducted using one-way ANOVA of AUC (* $p<0.05$, **$p<0.01$, ***$p<0.001$, ****$p<0.0001$).

397 **JAK-STAT inhibitor alters IFNε-mediated reduction of viral replication.**

398 To confirm that IFNε was signalling via the classical type I IFN signal induction pathway (IFNAR-
399 JAK-STAT) in airway epithelial cells, BEAS-2B (**Figure 6A-B**) and A549 (**Figure 6C-D**) cells were pre-
400 treated with the JAK inhibitor Ruxolitinib for 2 h prior to rhIFNε (**Figure 6A, C**) and rhIFNβ1 (**Figure**
401 **6B, D**) pre-treatment (100 ng/mL). Pre-treatment with Ruxolitinib eliminated the reduction in viral
402 replication with rhIFNε pretreatment in BEAS-2B cells (**Figure 6A**). A similar trend was seen for
403 rhIFNβ1-pre-treated BEAS-2Bs (**Figure 6B**), although the concentration of Ruxolitinib used was
404 not sufficient to completely block rhIFNβ1 signalling at 100 ng/mL. A549 cells did not produce a
405 significant reduction in viral replication with rhIFNε treatment as described above (**Figure 6C)**.
406 However, pre-treatment of A549 cells with 100 ng/mL of rhIFNβ1 or rhIFNβ1 did result in a
407 significant reduction in viral replication (**Figure 6D**). These results confirm the increased potency
408 of rhIFNβ1 compared to rhIFNε at 100 ng/mL but that, like rhIFNβ1, rhIFNε utilises the JAK-STAT
409 pathway to exert its antiviral effect against RSV.

410

411

412

413

414

415

416

417

418

419

420

421

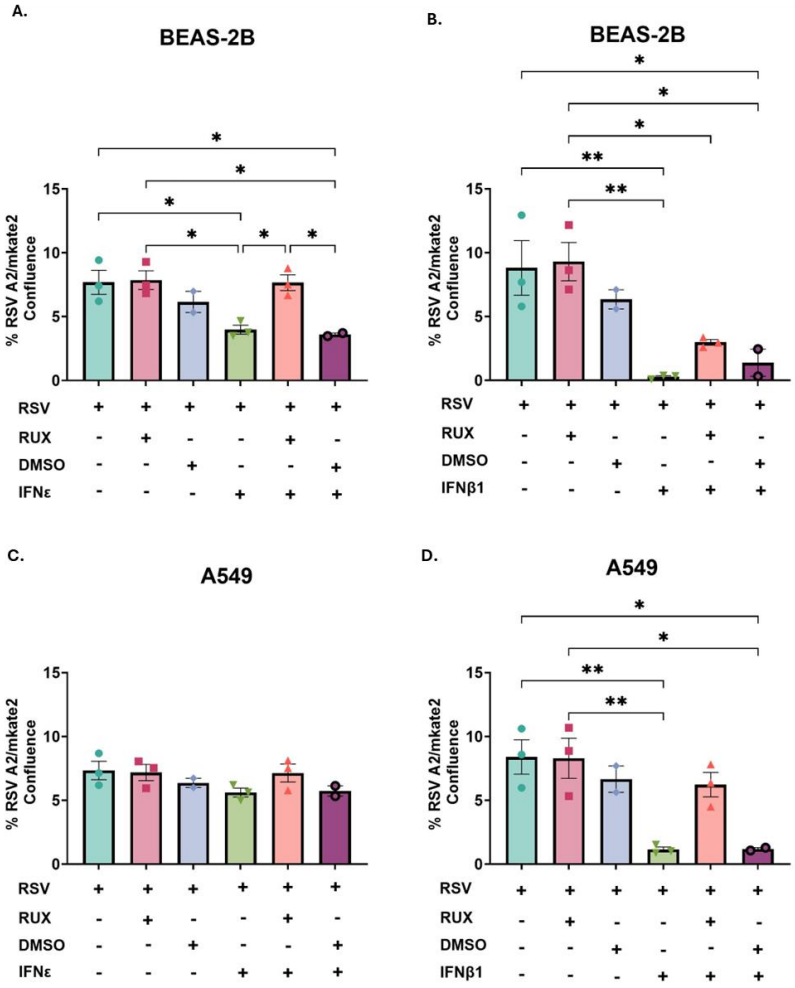

Figure 6. JAK-STAT inhibitor alters IFNε-mediated reduction of viral replication. BEAS-2B and A549 cells were pre-treated with Ruxolitinib (INCB018424, Selleck Chemicals) or DMSO (2.5 μM) for 2 h before 16 h IFNε (**A-B**), and IFNβ1 (**C-D**) pre-treatment (100 ng/mL). Cells were then infected with RSV (RSV-A2/mKate2) (MOI=0.1). At 24 hpi BEAS-2B (**A**, **C**) and A549 (**B**, **D**) cells mean % fluorescence ratio was measured using the brightfield and red fluorescence channels of the Celigo Imaging Cytometer (Nexcelom). Data presented as % fluorescence ratio for mean of triplicate technical replicates (±SEM) for n=3 independent experiments for RSV, RSV+RUX, RSV+IFNε and RSV+RUX+IFNε. Data presented as % fluorescence ratio of triplicate technical replicates for (±SEM) n=2 independent experiments for RSV+DMSO and RSV+DMSO+IFNε. Statistical analysis was conducted using one-way ANOVA (* $p<0.05$ **$p<0.01$).

433 **Differential ISG expression kinetics following rhIFNε, rhIFNλ1, and rhIFNβ1 treatment.**

434 In our hands, IFNε was capable of inhibiting RSV replication only at early time points post-
435 infection suggesting that the expression of downstream antiviral restriction factors may be
436 transient. To assess if any differences were evident in the magnitude and expression kinetics of
437 downstream antiviral restriction factors with rhIFNε treatment compared to rhIFNβ1 and rhIFNλ1,
438 RT-qPCR was conducted on RNA extracted from BEAS-2B cells treated with rhIFNε, rhIFNλ1 and
439 rhIFNβ1 (100 ng/mL) (**Figure 7A-F**). rhIFNε induced well known antiviral proteins, such as *MX1*
440 (**Figure 7A**), *ISG15* (**Figure 7B**), *IFIT1* (**Figure 7C**) and *RSAD2* (**Figure 7D**). Similarly, IFNε also
441 induced type I IFN-associated pro-inflammatory genes, such as *IRF1* (**Figure 7E**), and *CXCL10*
442 (**Figure 7F**), which were previously reported to be induced only at low levels and transiently by
443 rhIFNλ1 or other type III IFNs [38]. rhIFNε possessed unique ISG expression kinetics, with
444 expression peaking early (4 h post-treatment), in comparison to rhIFNβ1, which induced a more
445 potent and enduring response, and rhIFNλ1, which induced a slower yet incrementally increasing
446 response through 24 h post-treatment. These results demonstrate that rhIFNε can induce a
447 typical pro-inflammatory type I IFN antiviral gene signature in airway epithelial cells but that
448 temporal expression of downstream ISGs is transient compared to rhIFNβ1 and rhIFNλ1
449 treatment.

450

451

452

453

454

455

456

457

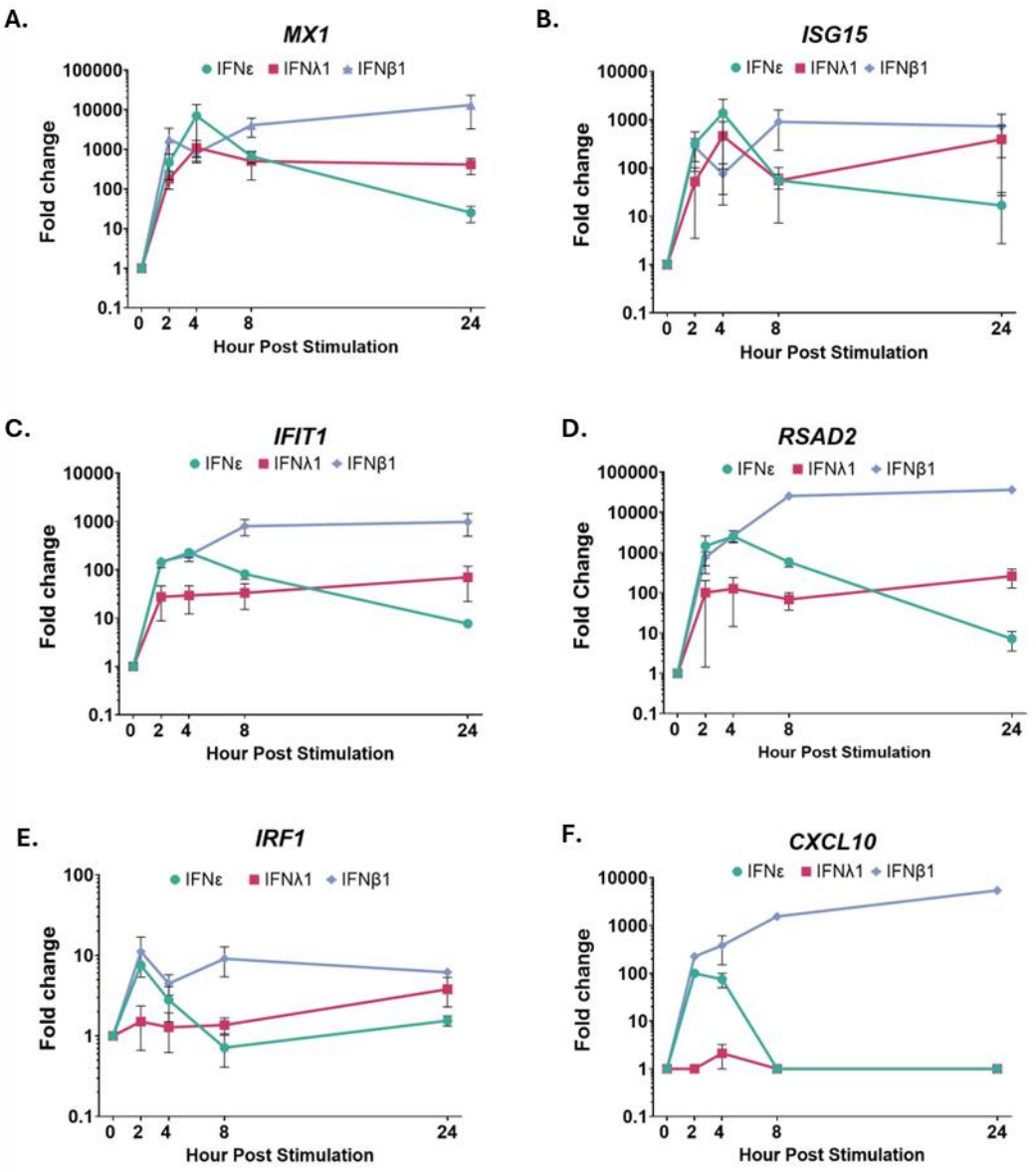

Figure 7. Differential induction of antiviral and pro-inflammatory ISGs by IFNε. BEAS-2B cells were treated with IFNε, IFNλ1 or IFNβ1 (100 ng/ml) and total RNA was extracted immediately from untreated (t=0) and at indicated time points post-stimulation. RNA was subjected to RT-qPCR analysis of *IFIT1*, *ISG15*, *MX1, RSAD2, IRF1 and CXCL10* expression (ROCHE, Lightcycler 480). Graphs show relative ratio values for antiviral ISGs (**A**) *MX1*, (**B**) *ISG15*, (**C**) *IFIT1,* (**D**) *RSAD2 and pro-inflammatory ISGs* (**E**) *IRF1* and (**F**) CXCL10, normalised using *YWHAZ*, *IPO8* and *TBP* as housekeeping genes. Data presented (**A**-**D**) are mean of duplicate technical replicates (±SEM) fold change from mock for n=3 independent experiments and data presented (**E**-**F**) are mean of duplicate technical replicates (±SEM) fold change from mock for n=2 independent experiments.

466 **Discussion**

467 Conflicting data exists surrounding the role of IFN responses during RSV infection, particularly
468 among those most vulnerable to severe RSV-related disease, infants aged 6 weeks to 6 months
469 of life. Most of what is known describe the "classical" type I (IFNβ1 and IFNα's) and type III (IFNλ1-
470 4) IFNs [39, 40]. However, little is understood about the "non-classical" IFN subtypes, such as
471 IFNε. Previously we exploited a unique cohort of primary paediatric airway epithelial cell samples
472 derived from the same healthy infants at birth and 1 year, to explore the development of innate
473 immune responses to RSV infection in the first year of life (unpublished data, Groves HE, McCabe
474 M, Coey J, Broadbent L, Guo-Parke H, Lopez Campos G, et al). We present here the differential
475 expression of *IFNE* with chronological age, between healthy newborn and 1-year infants, both
476 endogenously and following RSV infection in WD-PNECs cultures. This timespan coincides with
477 those infants with high susceptibility rates to severe RSV-related disease (newborn) and those
478 with lower frequencies of severe infection (1 year). Previous studies have reported endogenous
479 and infection-induced *IFNE* expression in both the upper and lower respiratory tracts in humans
480 and other mammals, with variations in expression linked to age and disease severity [24, 28, 29,
481 41, 42]. IFNε is conserved across various mammalian species [24, 43–46] but is a pseudogene
482 in species susceptible to infections that are relevant to this study [47–49], alluding to a
483 evolutionarily significant mucosal function. Collectively, these data suggest that IFNε may play a
484 protective role in the respiratory epithelium during early-life viral infection and elevated levels in
485 infants may be an indication of an improved ability to curtail and/or resolve infection.

486 As epithelial cells are the primary target of RSV infection *in vivo*, we assessed the expression of
487 *IFNE* in immortalised epithelial cell lines commonly used to model RSV infection. *IFNE* was
488 endogenously expressed at low levels in all cell lines tested. Recently, Martínez-Espinoza *et al*
489 described increased *IFNE* expression during infection with RSV and hMPV, with peak *IFNE*
490 expression at 48 hpi in A549 cells for both viruses [41]. We did not see this increase in *IFNE*

491 expression with RSV infection. This discrepancy may be due to various factors, including
492 differences in cell culturing conditions, viral strains used, assays performed, and other
493 experimental variables between authors. Our observations are consistent with its reported
494 unstimulated endogenous expression within the epithelium of the FRT and male reproductive
495 tract in humans and mice [21, 22, 50–52]. However, we did observe an increase in *IFNE*
496 expression within our RSV-infected WD-PNEC cultures, mirroring the increase Martinez-Espinoza
497 *et al* reported within human bronchial airway epithelial cells 3-5 days post RSV-infection [41].
498 Notably, Martínez-Espinoza *et al* suggested that RSV and hMPV induced *IFNE* expression in A549
499 cells via RIG-I, with contributions from MDA5 [41]. This suggests that viral RNA plays a role in the
500 induction of *IFNE* during active infection. The endogenous expression of *IFNE* is conserved across
501 multiple mucosal sites, concentrated primarily in the epithelial cells lining these surfaces.
502 Consequently, it may be regulated by distinct stimuli in a cell/tissue-specific manner, possibly by
503 distinct cell populations in these sites which fluctuate with tissue-specific stimuli. However, no
504 studies have been published regarding IFNε's role in human respiratory epithelium on a single-
505 cell level, and further work needs to be conducted regarding *IFNE* induction and regulation in
506 more physiologically relevant primary human airway epithelial models.

507 As a result of *IFNE's* endogenous epithelial expression, further investigation was prompted
508 regarding its possible contribution to localised antiviral activity. We showed that rhIFNε provided
509 antiviral protection against EMCV infection in BEAS-2B and A549 cells, consistent with similar
510 antiviral effects observed in cervical WISH cells [25]. Martínez-Espinoza *et al* demonstrated the
511 antiviral activity of rhIFNε against RSV and hMPV in A549 cells [41], which were shown to be highly
512 permissive to RSV infection [53]. Therefore, we chose to assess the antiviral properties of rhIFNε
513 in multiple respiratory cell lines. Pre-treatment with rhIFNε resulted in a significant dose-
514 dependent reduction in BEAS-2B and HEp-2 cell lines. BEAS-2B cells were observed to express
515 high levels of transcription factors and antiviral ISGs upon RSV infection and multiple IFN subtype
516 treatment, indicating a strong response to rhIFNε [53]. We did not observe a significant reduction

517 in virus fluorescence in A549 and AAT cells, when treated with 100 ng/mL of rhIFNε, consistent
518 with Martínez-Espinoza *et al.*, who found that at least 250 ng/mL was needed for a significant
519 effect on RSV fluorescence or titres in A549 cells [41]. In addition, prototypic lab-adapted strains,
520 such as RSV A2/mkate2, have been reported to result in greater cytopathogenesis and induce
521 greater concentrations of proinflammatory cytokines in the respiratory epithelium [33].
522 Therefore, we also chose to assess the antiviral activity of rhIFNε against a low passage clinical
523 isolate of RSV, which more accurately reflects RSV infection *in vivo*. We found that IFNε
524 pretreatment of BEAS-2B cells was antiviral against the clinical isolate RSV BT2a, with a
525 significant reduction in infectious viral release at 24 hpi. However, without being replenished, this
526 antiviral effect was quickly lost as the infection progressed. BEAS-2B cells were selected as the
527 representative cell line due to their significant reduction in RSV A2/mKate2 infection following
528 100 ng/mL rhIFNε pretreatment and their non-cancerous immortalized state. Our data
529 emphasizes the importance of cell line selection in studying viral IFN sensitivity, especially for
530 lesser-understood IFN subtypes and suggests that while IFNε may not be the primary defender
531 against viral infection in epithelial cells, they support its potential role as an endogenous antiviral
532 mucosal defence cytokine.

533 The relative antiviral activities of each IFN were reflected in their IC_{50} values. Our data indicated
534 that rhIFNε was ~3-fold less potent than rhIFNλ1 and ~38-fold less potent than rhIFNβ1, similar
535 to those described for recombinant mouse IFNε (rmIFNε) against EMCV in WISH cells [25].
536 Interestingly, the IC_{50} concentration of rhIFNε and 100 ng/mL was sufficient to reduce viral
537 replication under pretreatment and treatment-at-infection conditions, but not with treatment 2 h
538 post RSV infection in BEAS-2B cells. However, its inability to provide protection against infection
539 when added post-RSV infection most likely reflects its reduced antiviral potency and RSV's
540 recognised ability to efficiently modulate IFN responses [54]. This is consistent with data showing
541 a reduction in Zika virus replication in HRT8 cells with rmIFNε pretreatment, but not post-
542 infection [50]. As expected, RSV was also able to antagonise IFNβ1's antiviral activity when added

543 post-infection at its IC_{50} concentration, as IFNε and IFNβ1 share the same signalling pathway.
544 However, when added 2 h post-RSV infection at 100 ng/mL rhIFNβ1 was able to reduce viral
545 replication significantly, most likely reflecting rhIFNβ1's greater potency. As anticipated the
546 antiviral activity of rhIFNβ1 consistently superseded rhIFNε when added before, after or
547 simultaneously with rhIFNε. Like IFNβ1, IFNε possesses a greater affinity for the IFNAR1 chain
548 [25]. However, IFNε binds to IFNAR1 at a much lower affinity than IFNβ1 (100-1000-fold), which
549 may partly explain the increased antiviral capacity of IFNβ1 in this context [25].

550 Infection with the related virus rSeV/eGFP confirmed that IFNε's antiviral effect was not restricted
551 to RSV, with the greatest reduction in rSeV/eGFP fluorescence also observed within BEAS-2B
552 cells. However, we did not observe an antiviral effect against the SARS-CoV-2 Delta variant in AAT
553 cells at the very high dose tested (100 ng/mL), a variant that was previously described to have
554 increased sensitivity to IFNs [55–58]. To our knowledge, this is the first report demonstrating
555 SARS-CoV-2's insensitivity to rhIFNε [59]. Although our results suggest that rhIFNε was not
556 effective in altering SARS-CoV-2 infection, it is important to note that we used a modified
557 immortalized cell line highly susceptible to SARS-CoV-2 infection. Further studies in a more
558 physiologically relevant nasal epithelial model are required, given evidence that IFNε may
559 influence age-related responses to SARS-CoV-2 [29, 30]. It is possible that during SARS-CoV-2
560 infection, IFNε possess functions beyond direct antiviral activity, as suggested by its wider
561 immunomodulatory functions [60]. Overall, our data demonstrate that respiratory viruses
562 possess differential sensitivities to rhIFNε restriction and emphasise the importance of assessing
563 the antiviral capacity against multiple virus families.

564 Our data using a JAK-STAT signalling inhibitor confirmed that IFNε signals through this pathway to
565 exert its antiviral activity against RSV. These data provided the rationale to explore the magnitude
566 and kinetics of the induction of downstream ISGs with rhIFNε treatment. Recently, IFNε was
567 shown to induce common ISGs upregulated during RSV infection [41]. Our data showed that

568 rhIFNε treatment induced a unique ISG expression pattern with expression of four antiviral ISGs
569 associated with RSV infection (*MX1*, *ISG15*, *IFIT1* and *RSAD2*) peaking at 4 h post-stimulation.
570 IFNε's transient induction pattern was consistent with that observed against ZIKV infection in
571 human FRT cell lines [50] and this rapid transient ISG induction may be reflective of its short-term
572 reduction in viral titre at 24 hpi in BEAS-2B cells, but not at later time points. Furthermore, rhIFNε,
573 like rhIFNβ1, induced the expression of the transcription factor *IRF1* and the chemokine *CXCL10*.
574 rhIFNλ1 treatment did not induce *IRF1* or *CXCL10* expression to the same magnitude compared
575 to rhIFNε and rhIFNβ1. Rapid increased *IRF1* and *CXCL10 expression* are considered type I IFN-
576 associated [38]. However, type III IFNs were shown to induce *IRF1* and *CXCL10* expression at
577 lower levels [38]. Together our results demonstrated that rhIFNε can induce a strong classical
578 type I antiviral gene signature in airway epithelial cells but its potency and expression kinetics are
579 distinct compared to rhIFNβ1 and rhIFNλ1.

580 IFNε's unique low-level endogenous expression, its reduced potency, and transient ISG
581 expression kinetics, may strike a balance between the beneficial effects of type I IFN and
582 minimizing the tissue toxicity associated with its presence [61]. The question remains whether
583 the endogenous expression of IFNε results in a continuously primed airway epithelium, creating
584 an endogenous barrier to infection. If so, IFNε or the ISGs it induces could be leveraged as
585 potential biomarkers to identify those children at increased risk of severe disease in which no
586 high-risk factors have been identified (6 weeks and 6 months). Could the unique properties of
587 IFNε be further harnessed as an antiviral to non-destructively boost protective responses to
588 infection? Further work is required to explore IFNε's ability to boost or improve innate immune
589 responses within primary airway epithelial cell cultures.

590 **Conclusion**

591 IFNε is a highly conserved type I IFN expressed at multiple mucosal surfaces and is recognised
592 for its antimicrobial abilities in the FRT. We demonstrated differential expression of *IFNE* with age

593 and RSV infection in human nasal epithelial cells and confirmed its antiviral activity against a
594 clinical isolate of RSV. Although less potent than rhIFNβ1 or rhIFNλ1, rhIFNε's unique ISG
595 expression kinetics at 100 ng/mL and mild inflammatory profile suggest it may play a role in
596 mitigating RSV infection in airway epithelium. Reduced IFNε expression in newborns may
597 partially explain their heightened vulnerability to RSV, presenting an opportunity for therapeutic
598 interventions. Further studies are needed to explore IFNε's potential as an antiviral therapy or
599 prognostic tool for early-life respiratory infections.

600

601

602

603

604

605

606

607

608

609

610

611

612

613

614

615

616

617

618 **References**

619 [1] Li Y, Wang X, Blau DM, et al. Global, regional, and national disease burden estimates of
620 acute lower respiratory infections due to respiratory syncytial virus in children younger
621 than 5 years in 2019: a systematic analysis. *Lancet* 2022; 399: 2047–2064.

622 [2] Hammitt LL, Dagan R, Yuan Y, et al. Nirsevimab for Prevention of RSV in Healthy Late-
623 Preterm and Term Infants. *N Engl J Med* 2022; 386: 837–846.

624 [3] Drysdale SB, Cathie K, Flamein F, et al. Nirsevimab for Prevention of Hospitalizations
625 Due to RSV in Infants. *N Engl J Med* 2023; 389: 2425–2435.

626 [4] Ares-Gómez S, Mallah N, Santiago-Pérez M-I, et al. Effectiveness and impact of universal
627 prophylaxis with nirsevimab in infants against hospitalisation for respiratory syncytial
628 virus in Galicia, Spain: initial results of a population-based longitudinal study. *Lancet*
629 *Infect Dis* 2024; 24: 817–828.

630 [5] Walsh EE, Pérez Marc G, Zareba AM, et al. Efficacy and Safety of a Bivalent RSV Prefusion
631 F Vaccine in Older Adults. *N Engl J Med* 2023; 388: 1465–1477.

632 [6] Kampmann B, Madhi SA, Munjal I, et al. Bivalent Prefusion F Vaccine in Pregnancy to
633 Prevent RSV Illness in Infants. *N Engl J Med* 2023; 388: 1451–1464.

634 [7] Hall CB, Weinberg GA, Iwane MK, et al. The burden of respiratory syncytial virus infection
635 in young children. *N Engl J Med* 2009; 360: 588–598.

636 [8] MacDonald NE, Hall CB, Suffin SC, et al. Respiratory Syncytial Viral Infection in Infants
637 with Congenital Heart Disease. *N Engl J Med* 1982; 307: 397–400.

638 [9] Chaw PS, Wong SWL, Cunningham S, et al. Acute Lower Respiratory Infections
639 Associated With Respiratory Syncytial Virus in Children With Underlying Congenital
640 Heart Disease: Systematic Review and Meta-analysis. *J Infect Dis* 2020; 222: S613–S619.

641 [10] Rose EB, Dahl RM, Havers FP, et al. Respiratory Syncytial Virus-Associated
642 Hospitalizations in Children With Neurological Disorders, 2006-2015. *J Pediatric Infect*
643 *Dis Soc* 2021; 10: 951–957.

644 [11] Moyes J, Cohen C, Pretorius M, et al. Epidemiology of Respiratory Syncytial Virus–
645 Associated Acute Lower Respiratory Tract Infection Hospitalizations Among HIV-Infected
646 and HIV-Uninfected South African Children, 2010–2011. *J Infect Dis* 2013; 208: S217–
647 S226.

648 [12] Kristensen K, Hjuler T, Ravn H, et al. Chronic Diseases, Chromosomal Abnormalities,
649 and Congenital Malformations as Risk Factors for Respiratory Syncytial Virus
650 Hospitalization: A Population-Based Cohort Study. *Clin Infect Dis* 2012; 54: 810–817.

651 [13] Shi T, Vennard S, Mahdy S, et al. Risk Factors for Poor Outcome or Death in Young
652 Children With Respiratory Syncytial Virus–Associated Acute Lower Respiratory Tract
653 Infection: A Systematic Review and Meta-Analysis. *J Infect Dis* 2022; 226: S10–S16.

654 [14] Chaw PS, Hua L, Cunningham S, et al. Respiratory Syncytial Virus-Associated Acute
655 Lower Respiratory Infections in Children With Bronchopulmonary Dysplasia: Systematic
656 Review and Meta-Analysis. *J Infect Dis* 2020; 222: S620–S627.

657 [15] Becker S, Soukup J, Yankaskas JR. Respiratory syncytial virus infection of human primary
658 nasal and bronchial epithelial cell cultures and bronchoalveolar macrophages. *Am J*
659 *Respir Cell Mol Biol* 1992; 6: 369–374.

660 [16] Villenave R, Thavagnanam S, Sarlang S, et al. In vitro modeling of respiratory syncytial
661 virus infection of pediatric bronchial epithelium, the primary target of infection in vivo.
662 *Proc Natl Acad Sci U S A* 2012; 109: 5040–5045.

663 [17] Zhang L, Peeples ME, Boucher RC, et al. Respiratory syncytial virus infection of human
664 airway epithelial cells is polarized, specific to ciliated cells, and without obvious

665 cytopathology. *J Virol* 2002; 76: 5654–5666.

666 [18] Stanifer ML, Guo C, Doldan P, et al. Importance of Type I and III Interferons at Respiratory
667 and Intestinal Barrier Surfaces. *Front Immunol* 2020; 11: 608645.

668 [19] Mesev E V, LeDesma RA, Ploss A. Decoding type I and III interferon signalling during viral
669 infection. *Nat Microbiol* 2019; 4: 914–924.

670 [20] Taveras J, Garcia-Maurino C, Moore-Clingenpeel M, et al. Type III Interferons, Viral Loads,
671 Age, and Disease Severity in Young Children with Respiratory Syncytial Virus Infection. *J*
672 *Infect Dis* 2023; 227: 61–70.

673 [21] Hardy MP, Owczarek CM, Jermiin LS, et al. Characterization of the type I interferon locus
674 and identification of novel genes. *Genomics* 2004; 84: 331–345.

675 [22] Fung KY, Mangan NE, Cumming H, et al. Interferon-ε protects the female reproductive
676 tract from viral and bacterial infection. *Science* 2013; 339: 1088–1092.

677 [23] Bourke NM, Achilles SL, Huang SU-S, et al. Spatiotemporal regulation of human IFN-ε
678 and innate immunity in the female reproductive tract. *JCI insight*; 7. Epub ahead of print
679 September 2022. DOI: 10.1172/jci.insight.135407.

680 [24] Demers A, Kang G, Ma F, et al. The mucosal expression pattern of interferon-ε in rhesus
681 macaques. *J Leukoc Biol* 2014; 96: 1101–1107.

682 [25] Stifter SA, Matthews AY, Mangan NE, et al. Defining the distinct, intrinsic properties of
683 the novel type I interferon, IFNϵ. *J Biol Chem* 2018; 293: 3168–3179.

684 [26] de Geus ED, Volaric JS, Matthews AY, et al. Epithelially Restricted Interferon Epsilon
685 Protects Against Colitis. *Cell Mol Gastroenterol Hepatol* 2024; 17: 267–278.

686 [27] Harris BD, Schreiter J, Chevrier M, et al. Human interferon-ϵ and interferon-κ exhibit low
687 potency and low affinity for cell-surface IFNAR and the poxvirus antagonist B18R. *J Biol*

688 *Chem* 2018; 293: 16057–16068.

689 [28] Thwaites RS, Coates M, Ito K, et al. Reduced Nasal Viral Load and IFN Responses in
690 Infants with Respiratory Syncytial Virus Bronchiolitis and Respiratory Failure. *Am J*
691 *Respir Crit Care Med* 2018; 198: 1074–1084.

692 [29] Pierangeli A, Gentile M, Oliveto G, et al. Comparison by Age of the Local Interferon
693 Response to SARS-CoV-2 Suggests a Role for IFN-ε and -ω. *Front Immunol* 2022; 13: 1–
694 10.

695 [30] Fracella M, Mancino E, Nenna R, et al. Age-related transcript changes in type I interferon
696 signaling in children and adolescents with long COVID. *Eur J Immunol* 2024; 54: 1–10.

697 [31] Groves HE, Guo Parke H, Broadbent L, et al. Characterisation of morphological
698 differences in well-differentiated nasal epithelial cell cultures from preterm and term
699 infants at birth and one-year. *PLoS One* 2018; 1–14.

700 [32] Broadbent L, Villenave R, Hong G-P, et al. In Vitro Modeling of RSV Infection and
701 Cytopathogenesis in Well-Differentiated Human Primary Airway Epithelial Cells (WD-
702 PAECs). In: Tripp RA, Jorquera P (eds) *Human Respiratory Syncytial Virus*. Springer, 2016,
703 pp. 199–139.

704 [33] Villenave R, O'Donoghue D, Thavagnanam S, et al. Differential cytopathogenesis of
705 respiratory syncytial virus prototypic and clinical isolates in primary pediatric bronchial
706 epithelial cells. *Virol J* 2011; 8: 43.

707 [34] Rémi V, Olivier T, Surendran T, et al. Cytopathogenesis of Sendai Virus in Well-
708 Differentiated Primary Pediatric Bronchial Epithelial Cells . *J Virol* 2010; 84: 11718–
709 11728.

710 [35] Bamford CGG, Broadbent L, Aranday-Cortes E, et al. Comparison of SARS-CoV-2
711 Evolution in Paediatric Primary Airway Epithelial Cell Cultures Compared with Vero-

712 Derived Cell Lines. *Viruses*; 14. Epub ahead of print February 2022. DOI:
713 10.3390/v14020325.

714 [36] Bamford CGG, Aranday-Cortes E, Filipe IC, et al. A polymorphic residue that attenuates
715 the antiviral potential of interferon lambda 4 in hominid lineages. *PLOS Pathog* 2018; 14:
716 e1007307.

717 [37] Guo-Parke H, Canning P, Douglas I, et al. Relative respiratory syncytial virus
718 cytopathogenesis in upper and lower respiratory tract epithelium. *Am J Respir Crit Care*
719 *Med* 2013; 188: 842–851.

720 [38] Forero A, Ozarkar S, Li H, et al. Differential Activation of the Transcription Factor
721 IRF1 Underlies the Distinct Immune Responses Elicited by Type I and Type III Interferons.
722 *Immunity* 2019; 51: 451-464.e6.

723 [39] Stephens LM, Varga SM. Function and modulation of type i interferons during respiratory
724 syncytial virus infection. *Vaccines* 2020; 8: 1–16.

725 [40] Broggi A, Granucci F, Zanoni I. Type III interferons: Balancing tissue tolerance and
726 resistance to pathogen invasion. *J Exp Med* 2019; 217: e20190295.

727 [41] Martínez-Espinoza I, Babawale PI, Miletello H, et al. Interferon Epsilon-Mediated Antiviral
728 Activity Against Human Metapneumovirus and Respiratory Syncytial Virus. *Vaccines*; 12.
729 Epub ahead of print October 2024. DOI: 10.3390/vaccines12101198.

730 [42] Fung KY, de Geus ED, Ying L, et al. Expression of Interferon Epsilon in Mucosal
731 Epithelium is Regulated by Elf3. *Mol Cell Biol* 2024; 44: 334–343.

732 [43] Chung O, Jung Y-E, Lee KW, et al. The Analyses of Cetacean Virus-Responsive Genes
733 Reveal Evolutionary Marks in Mucosal Immunity-Associated Genes. *Biochem Genet*
734 2022; 60: 2299–2312.

735 [44] Abdel-Fattah M, Saeed H, El-Shennawy L, et al. The Arabian camel, Camelus
736 dromedarius interferon epsilon: Functional expression, in vitro refolding, purification
737 and cytotoxicity on breast cancer cell lines. *PLoS One* 2019; 14: e0213880.

738 [45] Yang L, Xu L, Li Y, et al. Molecular and functional characterization of canine interferon-
739 epsilon. *J Interf cytokine Res Off J Int Soc Interf Cytokine Res* 2013; 33: 760–768.

740 [46] Fischer CD, Wachoski-Dark GL, Grant DM, et al. Interferon epsilon is constitutively
741 expressed in equine endometrium and up-regulated during the luteal phase. *Anim*
742 *Reprod Sci* 2018; 195: 38–43.

743 [47] Choo SW, Rayko M, Tan TK, et al. Pangolin genomes and the evolution of mammalian
744 scales and immunity. *Genome Res* 2016; 26: 1312–1322.

745 [48] Ahmad HI, Jameel L, Zahra Q, et al. Molecular Evolution of Interferon-Epsilon (IFNϵ)
746 Pseudogene Modulates Innate and Specific Antiviral Immunity in Manis javanica. *J Zool*
747 *Syst Evol Res*; 2023. Epub ahead of print 2023. DOI: 10.1155/2023/2949008.

748 [49] Shi W, Shi M, Que T-C, et al. Trafficked Malayan pangolins contain viral pathogens of
749 humans. *Nat Microbiol* 2022; 7: 1259–1269.

750 [50] Coldbeck-Shackley RC, Romeo O, Rosli S, et al. Constitutive expression and distinct
751 properties of IFN-epsilon protect the female reproductive tract from Zika virus infection.
752 *PLOS Pathog* 2023; 19: e1010843.

753 [51] Bourke NM, Mesiano S, Hertzog PJ. Spatiotemporal regulation of human IFNε and innate
754 immunity in the female reproductive tract.

755 [52] Wijayarathna R, de Geus ED, Genovese R, et al. Interferon epsilon is produced in the
756 testis and protects the male reproductive tract against virus infection, inflammation and
757 damage. *PLoS Pathog* 2024; 20: e1012702.

758 [53] Hillyer P, Shepard R, Uehling M, et al. Differential Responses by Human Respiratory
759 Epithelial Cell Lines to Respiratory Syncytial Virus Reflect Distinct Patterns of Infection
760 Control. *J Virol*; 92. Epub ahead of print August 2018. DOI: 10.1128/JVI.02202-17.

761 [54] Jin H, Zhou H, Cheng X, et al. Recombinant Respiratory Syncytial Viruses with Deletions
762 in the NS1, NS2, SH, and M2-2 Genes Are Attenuated in Vitro and in Vivo. *Virology* 2000;
763 273: 210–218.

764 [55] Guo K, Barrett BS, Morrison JH, et al. Interferon resistance of emerging SARS-CoV-2
765 variants. *Proc Natl Acad Sci U S A* 2022; 119: 1–8.

766 [56] Nchioua R, Schundner A, Klute S, et al. Reduced replication but increased interferon
767 resistance of SARS-CoV-2 Omicron BA.1. *Life Sci alliance*; 6. Epub ahead of print June
768 2023. DOI: 10.26508/lsa.202201745.

769 [57] Thorne LG, Bouhaddou M, Reuschl A-K, et al. Evolution of enhanced innate immune
770 evasion by SARS-CoV-2. *Nature* 2022; 602: 487–495.

771 [58] Reuschl A-K, Thorne LG, Whelan MVX, et al. Evolution of enhanced innate immune
772 suppression by SARS-CoV-2 Omicron subvariants. *Nat Microbiol* 2024; 9: 451–463.

773 [59] Bastard P, Gervais A, Le Voyer T, et al. Human autoantibodies neutralizing type I IFNs:
774 From 1981 to 2023. *Immunol Rev* 2024; 322: 98–112.

775 [60] Mayall JR, Horvat JC, Mangan NE, et al. Interferon-epsilon is a novel regulator of NK cell
776 responses in the uterus. *EMBO Mol Med* 2024; 16: 267–293.

777 [61] Rodero MP, Crow YJ. Type I interferon–mediated monogenic autoinflammation: The type
778 I interferonopathies, a conceptual overview. *J Exp Med* 2016; 213: 2527–2538.

779

780